

Spatial organisation affects the pathway to precipitation in simulated trade-wind convection

Jule Radtke¹, Raphaela Vogel¹, Felix Ament², and Ann Kristin Naumann³

¹Meteorological Institute, Center for Earth System Research and Sustainability, Universität Hamburg

²University Hamburg

³Max Planck Institute for Meteorology

September 19, 2023

Abstract

We investigate whether and how spatial organisation affects the pathway to precipitation in large-domain hectometer simulations of the North Atlantic trades. We decompose the development of surface precipitation (P) in warm shallow trade cumulus into a formation phase, where cloud condensate is converted into rain, and a sedimentation phase, where rain falls towards the ground while some of it evaporates. With strengthened organisation, rain forms in weaker updrafts from smaller cloud droplets so that cloud condensate is less efficiently converted into rain. At the same time, organisation creates a locally moister environment and modulates the microphysical conversion processes that determine the raindrops' size. This reduces evaporation and more of the formed rain reaches the ground. Organisation thus affects how the two phases contribute to P , but only weakly affects the total precipitation efficiency. We conclude that the pathway to precipitation differs with organisation and suggest that organisation buffers rain development.

1 **Spatial organisation affects the pathway to precipitation in**
2 **simulated trade-wind convection**

3 **Jule Radtke^{1,2}, Raphaela Vogel¹, Felix Ament¹, Ann Kristin Naumann^{3,1}**

4 ¹Meteorological Institute, Center for Earth System Research and Sustainability, Universität Hamburg, Germany

5 ²International Max Planck Research School on Earth System Modelling, Hamburg, Germany

6 ³Max Planck Institute for Meteorology, Hamburg, Germany

7 **Key Points:**

- 8 • The development of surface precipitation in simulated trade-wind convection is decomposed
9 into a formation and sedimentation phase
- 10 • As organisation strengthens, less cloud condensate is converted into rain, but more rain
11 reaches the ground as evaporation is suppressed
- 12 • Organisation affects rain formation by modulating the local moisture environment, cloud
13 vertical motion and microphysical properties

Corresponding author: Jule Radtke, jule.radtke@uni-hamburg.de

Abstract

We investigate whether and how spatial organisation affects the pathway to precipitation in large-domain hectometer simulations of the North Atlantic trades. We decompose the development of surface precipitation (P) in warm shallow trade cumulus into a formation phase, where cloud condensate is converted into rain, and a sedimentation phase, where rain falls towards the ground while some of it evaporates. With strengthened organisation, rain forms in weaker updrafts from smaller cloud droplets so that cloud condensate is less efficiently converted into rain. At the same time, organisation creates a locally moister environment and modulates the microphysical conversion processes that determine the raindrops' size. This reduces evaporation and more of the formed rain reaches the ground. Organisation thus affects how the two phases contribute to P , but only weakly affects the total precipitation efficiency. We conclude that the pathway to precipitation differs with organisation and suggest that organisation buffers rain development.

Plain Language Summary

Clouds in the trade-wind region organise into a variety of spatial patterns. We investigate how this spatial organisation influences rain development in simulations of trade-wind convection. We divide the formation of surface precipitation into two phases. In the first phase, rain forms from the collision of cloud droplets or the collection of cloud droplets by raindrops. In the second phase, rain falls towards the ground while some of the rain evaporates. Our study shows that as organisation strengthens, rain forms less efficiently, but a larger fraction of that rain reaches the ground as evaporation is reduced. Thus, organisation in the simulations affects the way surface rain is generated. Our analyses suggest that it does so by modulating the cloud vertical motion in which rain forms, the local moisture environment through which rain falls and the microphysical conversion processes.

1 Introduction

What makes it rain? Precipitation was often neglected in studies of trade-wind convection because it was assumed that the convection is too shallow and short-lived to form precipitation (Siebesma, 1998; Stevens, 2005). Although there was already ample evidence of precipitation in the trade-wind region shown by Byers and Hall (1955) or Short and Nakamura (2000), it was not until attention to the trades and its clouds increased due to their large contribution to uncertainty in cloud feedbacks and climate sensitivity (Bony & Dufresne, 2005; Vial et al., 2013) that a more nuanced picture of trade-wind convection settled. The Rain In Cumulus over the Ocean (RICO) campaign (Raubert et al., 2007) was key in substantiating that precipitation is frequent in the trades (Nuijens et al., 2009), and highlighted that precipitation was often observed with arc-like cloud structures reminiscent of cold pool outflows (Snodgrass et al., 2009). Subsequent studies confirmed that trade-wind convection organises into a variety of spatial structures — and that this often occurs in conjunction with precipitation development (Stevens et al., 2020; Denby, 2020; Bony et al., 2020; Schulz et al., 2021; Vogel et al., 2021; Radtke et al., 2022). How does spatial organisation influence the development of (surface) precipitation in the trades? In this study, we exploit realistic large-domain hectometer(hm)-scale simulations of the North Atlantic trades (Schulz & Stevens, 2023) to investigate whether and how spatial organisation affects the pathway to trade-cumulus precipitation.

Precipitation formation depends on dynamic, thermodynamic and microphysical interactions on different spatial and temporal scales. Due to the broad range of scales and processes involved, an understanding of rain formation and contributing processes remains challenging, even for warm, shallow trade cumulus. The representation of trade-cumulus precipitation among large-eddy simulations (LES) differs largely (vanZanten et al., 2011). An understanding of how spatial organisation relates to warm rain development could help interpret and reduce these differences. Organisation may affect how efficient rain forms and how much evaporates through modulating mesoscale circulations or the local moisture environment (Seifert & Heus, 2013; Narenpitak et al., 2021). Moreover, understanding the relationship between spatial organisation and precipitation may also be key to disentangle the mechanisms of organisation and explain its influence on the total cloud cover in the trades, a prerequisite to further constrain the climate feedback of the trades (Nuijens & Siebesma, 2019; Bony et al., 2020).

Analysing rain radar measurements upstream of Barbados taken during the EUREC⁴A field campaign (Hagen et al., 2021; Stevens et al., 2021), Radtke et al. (2022) show that while the occurrence of trade-wind precipitation is related to organised cells, the mean rain rate varies largely independently of the cells' *degree* of organisation. However, scenes with similar precipitation but different degrees of spatial organisation also differed in the moisture environment. Similarly, Yamaguchi et al. (2019) find that in idealized LES, shallow cumulus precipitation varies little, but the sizes and spatial distribution of clouds differ in response to large changes in the aerosol environment. Could spatial organisation be a mechanism to maintain precipitation in different environments, enabling or creating a different pathway to precipitation?

To answer this question on a process-level, we make use of large-domain hm-scale simulations of the North Atlantic trades that were run for the period January to February 2020 during the EUREC⁴A campaign (Bony et al., 2017; Stevens et al., 2021; Schulz & Stevens, 2023) and were designed to explore spatial organisation on the mesoscale (20-200km). We follow the method of Langhans et al. (2015) and Lutsko and Cronin (2018) and decompose the development of surface precipitation into two phases, (i) a formation phase, in which cloud condensate is converted into rain water, and (ii) a sedimentation phase, in which the formed rain water falls towards the ground while part of it evaporates. Sect. 2 describes the setup and microphysical scheme of the simulations and our analysis method. Sect. 3.1 shows that spatial organisation in scenes of $\mathcal{O}(100\text{km})$ influences how these two phases contribute to the development of trade-wind precipitation. Sect. 3.2 explains such behaviour and interprets it as a form of buffering, before we conclude in Sect. 4.

2 Methods

2.1 EUREC⁴A large-domain ICON hm-scale simulations

The simulations are conducted with the LES configuration of the ICOSahedral Non-hydrostatic (ICON) model (Dipankar et al., 2015). ICON solves the compressible Navier–Stokes equations on an unstructured grid as detailed in Zängl et al. (2015) and Dipankar et al. (2015). To explore mesoscale convective variability, the simulations are performed with a relatively fine hectometre-scale mesh over a large domain of $\mathcal{O}(1000\text{km})$ for an extended EUREC⁴A campaign period from 9 January to 19 February 2022. They are realistically forced with initial and boundary data from a

96 storm resolving simulation at 1.25-km grid spacing, which is in turn initialised and nudged at its
 97 lateral boundaries to the atmospheric analysis of the European Centre for Medium-Range Weather
 98 Forecasts (similar to Klocke et al., 2017). Here, we analyse a simulation with 625 m gridspacing that
 99 covers the western tropical Atlantic from 60.25–45.0 °W and 7.5–17.0 °N, spanning about 1650
 100 km in the east-west direction, and 1050 km in the north-south direction. In the vertical, 150 lev-
 101 els are used, resulting in 70 m and 85 m vertical resolution at 1000 m and 2000 m height, respectively.

102
 103 Schulz and Stevens (2023) show that this simulation reproduces differences in the mesoscale struc-
 104 ture underlying the canonical forms of trade cumulus organisation of Stevens et al. (2020), as well as
 105 variability in precipitation, which makes them a good starting point to investigate how the process
 106 of precipitation may vary with spatial organisation. A nested 312 m simulation does not show a sub-
 107 stantially greater skill in representing different cloud organisations or rain rates (Schulz & Stevens,
 108 2023) and shows the same qualitative behaviour in our analysis (not shown). We refer the reader
 109 to Schulz and Stevens (2023) for an in-depth observational evaluation and comparison of the simu-
 110 lations. In the supplementary material we summarise and discuss the evaluation of the simulation
 111 properties relevant for our work.

112
 113 In the simulations, turbulence is parameterised with the Smagorinsky scheme, microphysics with the
 114 two-moment mixed-phase bulk microphysics scheme of Seifert and Beheng (2006) and a cloud con-
 115 densation nuclei concentration of 130 cm^{-3} is prescribed. Warm rain is produced by autoconversion
 116 and accretion, defined following Seifert and Beheng (2001) as $\frac{\partial L_r}{\partial t}|_{au} \sim L_c^2 \bar{x}_c^2$ and $\frac{\partial L_r}{\partial t}|_{acc} \sim L_c L_r$,
 117 where L_r is rain water content, L_c cloud water content and $\bar{x}_c = \frac{L_c}{N_c}$ mean mass of cloud droplets
 118 with cloud droplet number concentration N_c . To quantify the production of rain, we recalculate the
 119 autoconversion and accretion rates from the instantaneous 3D model output of cloud water, rain
 120 water and cloud effective radius r_{eff} , from which the volume radius r_v is derived by $(r_v/r_{\text{eff}})^3 = 0.8$
 121 (Freud & Rosenfeld, 2012) to calculate the cloud droplets' mean mass. The 3D output is available
 122 every 3 h.

123 2.2 Investigating spatial organisation and the pathway to precipitation

124 We investigate spatial organisation in scenes of $4 \times 4^\circ$ (about $450 \times 450 \text{ km}$), an area extent similar to
 125 previous studies (Radtke et al., 2022; George et al., 2022). Figure 1a shows three scenes with differ-
 126 ent degrees of organisation as an example. To mask high ice clouds, scenes with outgoing longwave
 127 radiation $< 275 \text{ W m}^{-2}$ are excluded (changes in the threshold do not affect our qualitative results),
 128 as well as scenes with little precipitation $P < 0.01 \text{ mm h}^{-1}$. Here and if not indicated otherwise, we
 129 refer to domain mean values. In total about 2000 scenes are used in the analyses (about 7 scenes
 130 across the domain every 3 hours).

131
 132 Following Bretherton and Blossey (2017) and Narenpitak et al. (2021), we assess the degree of
 133 spatial organisation as mesoscale variability in the moisture field, which is closely connected to the
 134 cloud structure. First, the total water path, W_T , defined as the sum of vertically integrated wa-
 135 ter vapor, cloud condensate, and rain, is coarse-grained into tile sizes of $20 \times 20 \text{ km}^2$, representing
 136 variability associated with the mesoscale (Orlanski, 1975). Subsequently, the coarse-grained W_T is
 137 binned into quartiles and the difference between the fourth and first quartile is calculated as organ-
 138 isation metric $O_{\Delta W_T}$. This metric classifies the three example scenes from weakly organised (low

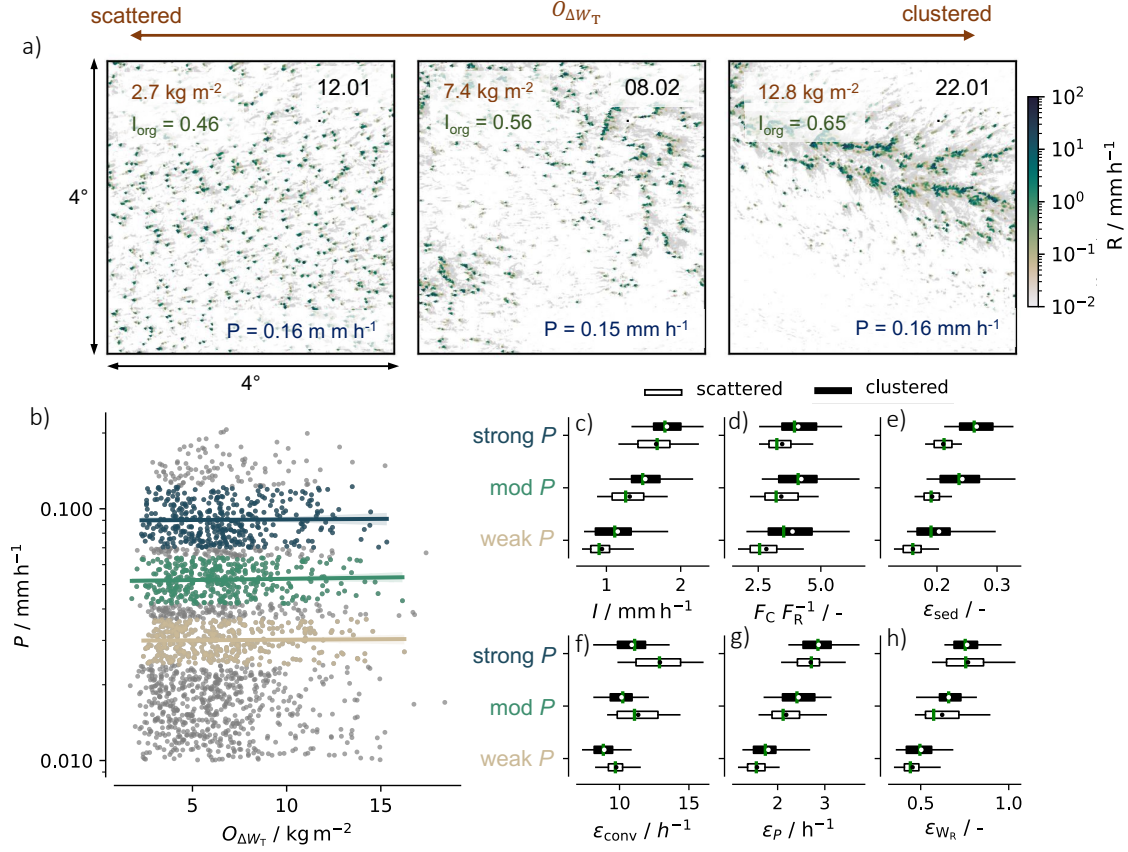


Figure 1. a) Three example scenes with similar scene-averaged precipitation P (i.e. rain amount, blue) but different degrees of organisation characterised by $O_{\Delta W_T}$ (orange) and the I_{ORG} (green). Colour shading denotes rain rate R . Grey shading denotes cloud albedo calculated from simulated cloud liquid water path. b) P as a function of $O_{\Delta W_T}$. Three different rain regimes with weak $P = (0.024, 0.037]$, mod $P = (0.042, 0.064]$ and high $P = (0.07, 0.12]$ are distinguished. c) Rain intensity I , d) cold pool fraction, F_C , per rain fraction, F_R , e) sedimentation efficiency ϵ_{sed} , f) conversion efficiency ϵ_{conv} , g) precipitation efficiency ϵ_P , and h) rain water loading efficiency $\epsilon_{WR} = \frac{W_R}{W_L}$, where W_R rain water path, shown for the three precipitation regimes, separated into a clustered ($O_{\Delta W_T} > 70^{\text{th}}$ percentile, filled bars) and scattered sample ($O_{\Delta W_T} < 30^{\text{th}}$ percentile, empty bars). The green line denotes the median, the dot the mean, the box the interquartile range and the whiskers denote the 5^{th} and 95^{th} percentile.

139 $O_{\Delta W_T}$) on the left, to more strongly organised (high $O_{\Delta W_T}$) on the right. This is consistent with
 140 a visual subjective classification of the cloud field, the nearest neighbour clustering technique I_{ORG}
 141 (Tompkins & Semie, 2017), and the cloud pattern classification of Stevens et al. (2020). According
 142 to this classification, the left scene depicts a Gravel pattern, characterised by scattered convection
 143 (low I_{ORG}), and the right scene a Fish pattern, characterised by more clustered convection (higher
 144 I_{ORG}). An overview and more in-depth discussion of different organisation metrics has recently been
 145 given by e.g. Janssens et al. (2021).

146

147 To investigate the pathway to trade-wind precipitation, we decompose the development of surface

rain following Langhans et al. (2015) and Lutsko and Cronin (2018) into (i) a formation phase and (ii) a sedimentation phase. In phase (i), warm rain initially forms by the merging of small cloud droplets, parameterised with the autoconversion rate. Additionally, rain is produced as falling rain-drops collect cloud droplets, parameterised with the accretion rate. Autoconversion dominates the formation of rain especially for young or short-lived clouds, while accretion contributes more to the formation of rain as clouds live longer and there is more time available for the collision-coalescence process to take place (Feingold et al., 2013). To quantify how efficient the formation of rain water is, we define a conversion efficiency

$$\epsilon_{\text{conv}} = \frac{C_{\text{R}}}{W_{\text{L}}}, \quad (1)$$

where $C_{\text{R}} = C_{\text{Auto}} + C_{\text{Acc}}$ with C_{Auto} and C_{Acc} denoting the vertically integrated autoconversion and accretion rates and W_{L} the cloud liquid water path. In phase (ii), the rain formed by autoconversion and accretion sediments towards the ground. During this process, some rain evaporates. The rain that does not evaporate reaches the ground as surface precipitation, P , so that we call

$$\epsilon_{\text{sed}} = \frac{P}{C_{\text{R}}} = 1 - \epsilon_{\text{evap}} \quad (2)$$

the sedimentation efficiency with ϵ_{evap} the evaporation efficiency. Please note that we do not refer to in-cloud sedimentation here, but, following Langhans et al. (2015) and Lutsko and Cronin (2018), we use sedimentation efficiency to refer to how much rain reaches the ground instead of evaporating.

The product of the conversion and sedimentation efficiencies describes how much cloud water in a given time interval is returned to the surface as precipitation, representing an overall precipitation efficiency ϵ_{P} , e.g. as used in Lau and Wu (2003):

$$\underbrace{\frac{P}{W_{\text{L}}}}_{\epsilon_{\text{P}}} = \underbrace{\frac{C_{\text{R}}}{W_{\text{L}}}}_{\epsilon_{\text{conv}}} \cdot \underbrace{\frac{P}{C_{\text{R}}}}_{\epsilon_{\text{sed}}}. \quad (3)$$

Said differently, the inverse of ϵ_{P} is the time it takes to remove all cloud water at the given precipitation rate, thus describing a typical residence time. It is to note that precipitation efficiency itself has no unique definition (e.g. Sui et al., 2020). Different results may emerge for different definitions and also depend on local versus domain-mean views. However, using an approximation of the condensation rate following Muller and Takayabu (2020) instead of liquid water path in (3) results in the same qualitative behaviour. Here, we mainly exploit precipitation efficiency and its decomposition into conversion and sedimentation efficiencies as a proxy for the pathway that precipitation development takes.

3 Results

3.1 The pathway to precipitation varies with organisation

The hm-scale simulations reproduce EUREC⁴A observations in that scene precipitation in the trades varies mainly independently of organisation (Radtke et al., 2022). This is depicted in the example scenes in Fig. 1a, which display a similar rain rate but vastly different degrees of organisation, and is more quantitatively shown in Fig. 1b. In the simulations, scene rain rates vary up to 0.2 mm h^{-1} as shown in Fig. 1b, which compares well to rain rates observed in the RICO (Nuijens et al., 2009) and EUREC⁴A campaign (Radtke et al., 2022). In the following, we will show whether also the pathway

186 to these rain rates is similar or in how far organisation affects how these rain rates are generated,
 187 and could thus be a process to maintain precipitation in different environments.

188
 189 To investigate this, we group our sample of scenes into three precipitation regimes, a weak, a
 190 moderate, and a strong precipitation regime, as visualised in Fig. 1b. In each regime, we define more
 191 organised scenes as $O_{\Delta W_T} > 70^{\text{th}}$ percentile and less organised scenes as $O_{\Delta W_T} < 30^{\text{th}}$ percentile,
 192 which we refer to as clustered and scattered sample, respectively. The conclusions are insensitive to
 193 the exact choice of threshold. This relative way of differentiating between more and less organised
 194 scenes is based on the simulated distribution of organisation, which will vary depending on how
 195 variable the large-scale conditions are and possibly which specific model is used.

196
 197 Fig. 1c shows that, instead of the mean rain rate, organisation tends to increase the rain inten-
 198 sity, which is again in line with observational studies of trade-wind (Radtke et al., 2022) and deep
 199 convection (Louf et al., 2019). That is, clustered convection produces the same amount of scene
 200 precipitation than scattered convection with more intense rain covering a smaller area. Detecting
 201 cold pools based on the calculation and criterion of a mixed layer height smaller than 400 m follow-
 202 ing Touzé-Peiffer et al. (2022), clustered scenes are also populated by more cold pools as shown in
 203 Fig. 1d, possibly associated with this increase in rain intensity. In clustered scenes, the cold-pool
 204 fraction is about four times greater than the rain fraction, whereas in scattered scenes it is about
 205 three times greater. These findings may already hint to an altered precipitation process in more
 206 organised compared to less organised scenes.

207
 208 We investigate the relationship between organisation and the conversion, sedimentation and to-
 209 tal precipitation efficiency (eq. 3), shown in Fig. 2a. Organisation maximises towards the lower right
 210 of the phase space, at low conversion and high sedimentation efficiencies. An increase in the degree
 211 of organisation is thus related to a decrease in how efficient cloud water is converted into rain and
 212 an increase in how efficient rain sediments as a greater fraction of rain reaches the ground instead
 213 of evaporating. The sedimentation efficiency varies between 0.1 and 0.3, emphasising that much of
 214 the rain evaporates, as reported by Naumann and Seifert (2016) or Sarkar et al. (2022). Fig. 2b
 215 shows that precipitation maximises towards the upper right of the same phase space, that is, at high
 216 sedimentation and conversion efficiencies. Within a precipitation regime, as shown in Fig. 1e, f, rain
 217 thus sediments more efficiently but forms less efficiently in clustered compared to scattered scenes.
 218 This behaviour is slightly enhanced in regimes with stronger precipitation.

219
 220 The product of the conversion and sedimentation efficiencies gives the overall precipitation efficiency,
 221 denoted in the contour lines in Fig. 2. Precipitation efficiency varies closely with precipitation and
 222 lies mostly between 1 h^{-1} and 3 h^{-1} . That one to three times the cloud liquid water path precipitates
 223 per hour emphasises the rapid turnover and rain formation in trade-wind clouds, which with tops
 224 greater than 2500 m "usually rain within half an hour" (Squires 1958). Because conversion efficiency
 225 decreases but sedimentation efficiency increases with organisation, contours of precipitation effi-
 226 ciency and organisation lie perpendicular to each other in Fig. 2a. This means that organisation and
 227 precipitation efficiency, like precipitation, vary mainly independently of each other. Composed
 228 on the three different precipitation regimes, Fig. 1g shows that precipitation efficiency compared
 229 to the conversion and sedimentation efficiency varies only weakly with organisation with a slight

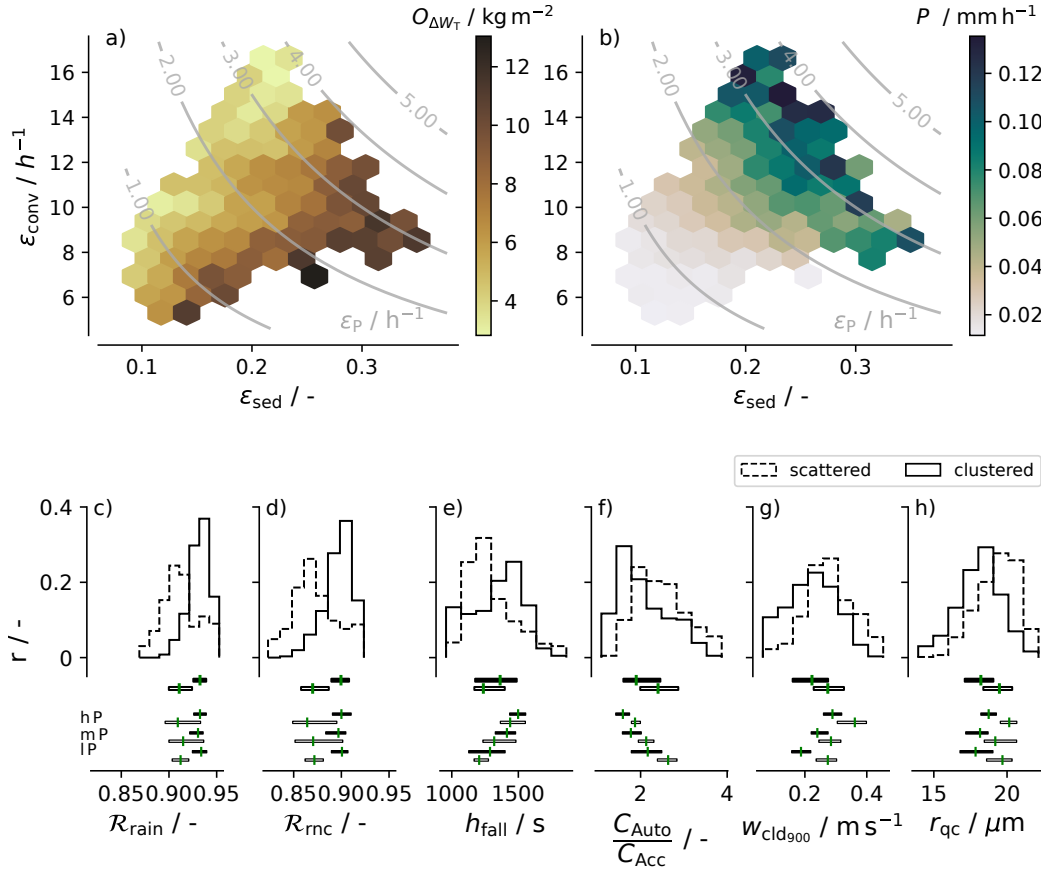


Figure 2. a) Degree of mesoscale organisation $O_{\Delta W_T}$ and b) precipitation P (shading) as a function of conversion efficiency ϵ_{conv} and sedimentation efficiency ϵ_{sed} . Contour lines denote precipitation efficiency from eq. (3). Relative frequency of c) rain-conditioned relative humidity \mathcal{R}_{rain} , d) rain-and-no-cloud-conditioned relative humidity \mathcal{R}_{rnc} , e) fall height h_{fall} , f) ratio of autoconversion C_{Auto} to accretion C_{Acc} , g) cloud-conditioned vertical velocity at 900 hPa $w_{cloud900}$ and h) mean cloud droplet radius r_{qc} for the scenes separated into scattered (dashed line, empty bars) and clustered (solid line, filled bars) convection and divided into three precipitation regimes (as in Fig. 1, hP denoting the high P regime, mP the mod P regime and lP the low P regime). Horizontal boxes denote the interquartile range, vertical lines the median.

230 tendency to increase with organisation. Analysing the ratio of rain water path to cloud water path
 231 instead of the ratio between precipitation and cloud liquid water path gives the same result (Fig. 1h).

232
 233 Our analysis thus suggests that organisation weakly affects precipitation efficiency in terms of how
 234 much cloud water precipitates on average, but changes the pathway to precipitation in terms of how
 235 the formation versus sedimentation phases contribute to the development of surface precipitation.
 236 Next, we investigate physical mechanisms behind this behaviour.

3.2 How does organisation affect the pathway to precipitation?

3.2.1 Sedimentation efficiency

The sedimentation efficiency describes how much rain reaches the ground instead of evaporating. Following Lutsko and Cronin (2018), we suggest that ϵ_{sed} should scale to a first approximation with the moisture environment through which the rain falls, or more explicitly with the saturation deficit, and the time it takes the rain to fall:

$$\epsilon_{\text{evap}} = 1 - \epsilon_{\text{sed}} \sim (1 - \mathcal{R}_{\text{rain}}) \cdot t_{\text{fall}} = (1 - \mathcal{R}_{\text{rain}}) \cdot \frac{h}{v}, \quad (4)$$

where $\mathcal{R}_{\text{rain}}$ is the averaged relative humidity the falling rain experiences, i.e. conditioned on pixels with rain water $q_r > 0.001 \text{ g kg}^{-1}$ (vanZanten et al., 2011), and t_{fall} the average fall time, which depends on the average fall height h and fall velocity v . The higher the saturation deficit or the longer the rain falls and thus has time to evaporate, the higher evaporation and the lower the amount of rain reaching the ground.

We hypothesise that organisation influences the moisture environment through which rain falls, since it manifests itself in an uneven (horizontal) distribution of moisture, as also used in our metric of organisation. Figure 2c shows that in the simulations, rain in clustered scenes indeed typically falls through a more humid environment with a lower saturation deficit than in scattered scenes. This is true for all precipitation regimes, with little variations in $\mathcal{R}_{\text{rain}}$ between precipitation regimes. We find that rain falls through a moister environment because the environment outside of or beneath clouds is closer to saturation (about 3%, Fig. 2d), not just because more rain may falls within than outside of clouds, e.g. due to different wind shears and cloud tilts. This is in line with the idea that clouds in more organised scenes develop preferentially in the parts of the domain with moister, more favourable thermodynamic conditions, e.g. preconditioned by former clouds (sometimes called mutual-protection hypothesis, Seifert & Heus, 2013) or established through enhanced moisture transport into anomalously moist patches by mesoscale circulations (Narenpitak et al., 2021; George et al., 2022). That way, clusters may form, clouds may be better protected from updraft buoyancy reduction through entrainment (Mapes & Neale, 2011; Becker et al., 2018), and less rain evaporates.

Besides the moisture environment, organisation could also influence the fall time of the rain drops by modulating the fall height or fall velocity (eq. 4). We define the fall height as average height where rain is produced by autoconversion and accretion, h_A . Analysing h_A shows that rain in clustered convection falls on average from slightly higher heights than in scattered convection (Fig. 2e), related to a tendency of clouds to grow deeper and inversion heights to increase with organisation (not shown). If the fall velocity stays unchanged, this would suggest that organisation slightly increases the time it takes for rain to fall to the ground, which would act to enhance, not to reduce evaporation in more strongly organised scenes.

For the mean fall velocity, multiple factors, e.g. the strength of up- and downdrafts and the raindrops' size is decisive. The raindrop size was not included in the model output but the way rain is produced, i.e. in how far autoconversion versus accretion dominate the formation of rain, may serve as a proxy for the raindrops' size. Figure 3a shows that in how far autoconversion versus accretion contributes to rain formation explains 79% of the variations in sedimentation efficiency. Because autoconversion produces initial "embryo" raindrops when cloud droplets merge, whereas accretion

280 is responsible for the growth of raindrops through further collection of cloud droplets, an increased
 281 contribution of accretion to rain formation indicates that raindrops have grown larger. Fig. 2f shows
 282 that in more organised scenes the contribution of accretion to rain formation is increased. Raindrops
 283 in more organised scenes are thus likely larger. Larger rain drops fall faster, reducing the fall time
 284 and hence evaporation.

285

286 When including, in addition to the relative importance of autoconversion and accretion, $\mathcal{R}_{\text{rain}}$ as
 287 additional predictor, 85% of the variations in sedimentation efficiency can be explained. Addition-
 288 ally including h_A does not explain further variations. Our analysis thus suggests, as illustrated in
 289 Fig. 4, that organisation reduces evaporation and increases the sedimentation efficiency because rain
 290 in more organised scenes is increasingly produced by accretion so that raindrops are larger and fall
 faster, through an environment that is moister.

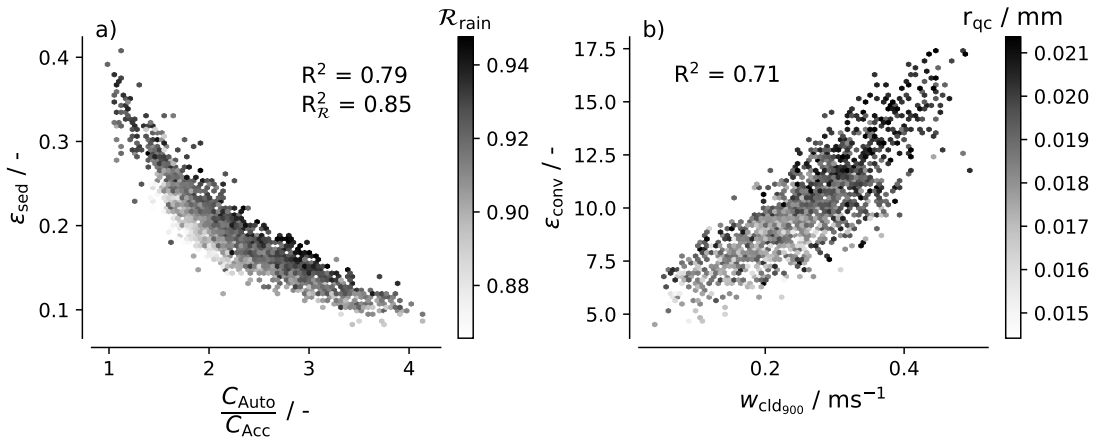


Figure 3. a) Sedimentation efficiency ϵ_{sed} as a function of the relative importance of autoconversion C_{Auto} and accretion C_{Acc} . Shading denotes the rain-conditioned relative humidity $\mathcal{R}_{\text{rain}}$. b) Conversion efficiency ϵ_{conv} as a function of cloud-conditioned vertical velocity at 900 hPa w_{cl_d900} . Shading denotes the mean cloud droplet radius r_{qc} .

291

292 3.2.2 Rain formation efficiency

293 Rain starts to form when sufficient cloud water has been produced and cloud droplets have grown to
 294 raindrop size (e.g. Seifert & Stevens, 2010). To initiate and grow cloud particles the air's saturation
 295 is important and influenced by thermodynamic conditions as well as vertical motions (Rogers &
 296 Yau, 1996).

297

298 In the simulations, organisation influences the clouds' vertical motion. Figure 2g shows that in
 299 clustered scenes the mean in-cloud vertical motion near cloud base, w_{cl_d900} (cloud-conditioned, i.e
 300 where cloud water $q_c > 0.01 \text{ g kg}^{-1}$, and at 900 hPa), is weaker than in more scattered scenes. This
 301 initially appears surprising. It can be attributed, in part, to the presence of stronger downdrafts,
 302 e.g. the 25th percentile of w_{cl_d900} is lower, and in part to weaker updrafts as the mean and median
 303 cloud upward motion is reduced (not shown). Bao and Windmiller (2021) found a similar decrease in

vertical motions with organisation in deep convection. Because organisation creates more favourable thermodynamic conditions for cloud and rain formation with a local increase in humidity (Fig. 2 c, d), this may allow clouds and rain to develop in less favourable dynamic conditions, i.e. at weaker mean upward motions. Additionally, the cloud population in more organised scenes could also consist of more long-lived, older clouds as indicated by the increased contribution of accretion to rain formation. In these, updrafts may have already started to weaken. Future analysis of the cloud lifecycle with respect to organisation may therefore potentially reconcile the apparent contradiction between the expected larger raindrops resulting from increased accretion and the presence of weaker updrafts.

More organised scenes also differ from less organised scenes in the mean cloud droplet radius. Fig. 2h shows that in clustered scenes, the mean cloud droplet radius is smaller by about $1.3 \mu\text{m}$ than in scattered scenes. From moderate to high precipitation, this difference increases, which is in line with the strong decrease in conversion efficiency at high precipitation. The smaller cloud droplet size in more organised scenes agrees with the weaker vertical motions. Besides, Cooper et al. (2013) showed that mixing and entrainment affects cloud droplet growth and the onset of precipitation. By changing the mixing characteristics of clouds, organisation might also influence the cloud droplets' size.

Figure 3b shows that 70% of the variations in conversion efficiency are explained by the mean vertical motion at cloud base, to which the mean cloud droplet size is correlated. To conclude and as illustrated in Fig. 4, our analyses suggest that organisation reduces the efficiency with which cloud water is converted into rain water because rain in clustered scenes forms in weaker updrafts that correlate with smaller mean cloud droplets. We hypothesise that this is because favourable thermodynamic conditions may compensate for weaker dynamic conditions and organisation may affect the lifetime as well as the mixing characteristics of the cloud population.

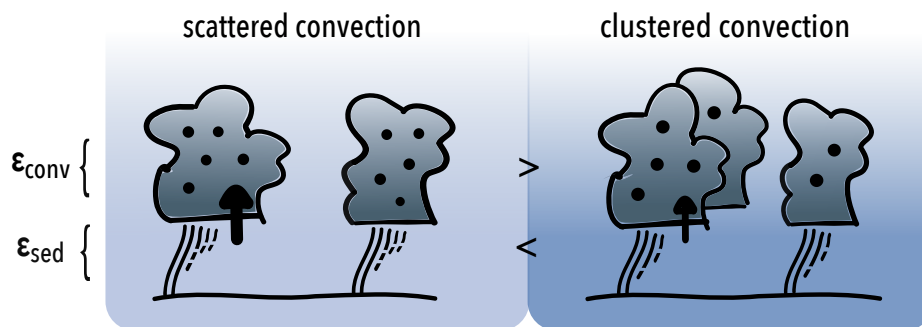


Figure 4. Conceptual illustration of the simulated pathway to surface precipitation in weakly (left) versus strongly (right) organised convection: For similar surface precipitation, as organisation strengthens, rain forms in a locally moister environment (shading) in weaker updrafts (arrow) and increasingly from accretion indicating larger raindrops (dots). As a consequence, evaporation is reduced, so that more rain reaches the ground compared to scattered convection (ϵ_{sed} is larger), but rain forms less efficiently (ϵ_{conv} is smaller), with both changes having a compensating, i.e. buffering effect on surface rain development.

3.2.3 Buffering

Organisation is associated with an increase in the sedimentation efficiency, but a decrease in the formation efficiency and thus influences rain development in an opposing or stabilising way. This may be interpreted as a form of buffering. Buffering as introduced in Stevens and Feingold (2009) denotes that if there are different pathways to reach the same final state, these buffer or stabilise the system against disruptions to any particular pathway. For example, cloud deepening as a dynamical response to increased droplet number concentration has been shown to buffer the microphysical suppression of precipitation (Seifert et al., 2015). Our analyses suggest that organisation has a stabilising, i.e. buffering, relationship to rain development, due to opposing effects on rain formation and sedimentation efficiency, as illustrated in Fig. 4. While in more scattered convection, rain development is characterised by efficient conversion of cloud water into rain water but also subsequent evaporation is strong, in more clustered convection, increased sedimentation efficiency compensates for a decreased conversion efficiency. These variations on the pathway to precipitation by organisation may be an additional explanation for why rain development is so common in the trades. They also offer an explanation for the observed (Radtke et al., 2022) and simulated independence between rain amount and organisation rather than a reinforcement.

Based on our results, we hypothesise that such buffering effect of organisation on rain development is related to (i) an interplay of thermodynamic and dynamic conditions and (ii) (life)time effects. Regarding (i), more favourable thermodynamic conditions may allow clouds to develop under less favourable dynamic conditions. Regarding (ii), the increased contribution of accretion to rain formation with organisation indicates longer-lived, older clouds, in agreement with the expectation of more sustained convection with organisation. In older, more mature clouds, the rain formation process had time to evolve (Feingold et al., 2013), so that raindrops may grow larger and fall out more efficiently, while updrafts may have already weakened so that further rain forms less efficiently.

4 Summary and conclusions

We exploit realistic large-domain hm-scale simulations of the North Atlantic trades to investigate whether and how organisation affects the pathway to trade-cumulus precipitation. We decompose the development of surface precipitation following Langhans et al. (2015) into a formation phase, where cloud condensate is converted to rain, and a sedimentation phase, where the formed rain falls to the ground while some of it evaporates. In the simulations, organisation affects how these two phases contribute to rain development, summarised schematically in Fig. 4.

With strengthened organisation, rain in the hm-scale simulations forms in and falls through a locally more humid environment. Additionally, rain is increasingly produced by accretion rather than autoconversion, which indicates that clouds live longer and raindrops grow larger. Larger raindrops, that fall through a more humid environment experience less evaporation, leading to an increase in the sedimentation efficiency. The relative importance of accretion and autoconversion explains 79% of the variations in sedimentation efficiency, increasing to 85% when including the rain-conditioned relative humidity as additional predictor. A locally more humid environment is in line with the idea that an increase in organisation is related to more humid patches in which clouds develop and which protect clouds from dilution and raindrops from evaporation. It may suggest that organisa-

tion also increases the efficiency with which cloud condensate is converted to rain. However, in more organised scenes rain forms in weaker updrafts (as in Bao & Windmiller, 2021), and from smaller cloud droplets. This leads to cloud water being less efficiently converted to rain, in agreement with radiative-convective equilibrium simulations by Lutsko and Cronin (2018). 71% of the variations in conversion efficiency are explained by the in-cloud vertical motion at cloud base, to which the cloud droplet size is correlated. Possibly because the thermodynamic environment is more favourable with organisation, less favourable dynamic conditions already allow for rain formation, or lifetime effects may play a role here. Both effects, the increase in sedimentation efficiency and the decrease in conversion efficiency, largely compensate, so that organisation does not substantially affect the total precipitation efficiency.

Our analyses suggest that organisation does not reinforce, but rather buffers rain development via opposing effects on the rain formation and sedimentation efficiencies. They offer an explanation for the observed and simulated independence between rain amount and organisation. While in less organised scenes rain development is characterised by efficient conversion of cloud condensate into rain, in more organised scenes more efficient sedimentation, as evaporation is suppressed, increasingly contributes to surface rain development. It remains to be shown in how far these results carry over to other models and observations. In our simulations, we conclude that the pathway to precipitation differs with spatial organisation.

Open Research Section

The simulation output is freely available and can be easily accessed via the EUREC⁴A-Intake catalog at <https://github.com/eurec4a/eurec4a-intake> as described at <https://howto.eurec4a.eu/simulations>. Detailed information about the simulations is given in Schulz and Stevens (2023).

Acknowledgments

This research was funded by the Deutsche Forschungsgemeinschaft (DFG, German Research Foundation) under Germany's Excellence Strategy – EXC 2037 'CLICCS - Climate, Climatic Change, and Society' – Project Number: 390683824, contribution to the Center for Earth System Research and Sustainability (CEN) of Universität Hamburg. EUREC4A was partly funded by the HALO priority program funded by the DFG - AM 308/11-1. Raphaela Vogel was partly funded by the European Research Council grant agreement 694768 (ERC Advanced Grant EUREC4A). We would like to thank Hauke Schulz for conducting the simulations. Computing resources were provided by the German Climate Computing Center (DKRZ). We also thank the editor as well as two anonymous reviewers for their valuable feedback. The authors declare no conflict of interest.

References

Bao, J., & Windmiller, J. M. (2021). Impact of Microphysics on Tropical Precipitation Extremes in a Global Storm-Resolving Model. *Geophysical Research Letters*, *48*(13), e2021GL094206. doi: 10.1029/2021GL094206

- 408 Becker, T., Bretherton, C. S., Hohenegger, C., & Stevens, B. (2018). Estimating Bulk Entrainment
409 With Unaggregated and Aggregated Convection. *Geophysical Research Letters*, *45*(1), 455–
410 462. doi: 10.1002/2017GL076640
- 411 Bony, S., & Dufresne, J.-L. (2005). Marine boundary layer clouds at the heart of tropical cloud
412 feedback uncertainties in climate models. *Geophysical Research Letters*, *32*(20). doi: 10.1029/
413 2005GL023851
- 414 Bony, S., Schulz, H., Vial, J., & Stevens, B. (2020). Sugar, Gravel, Fish, and Flowers: Dependence of
415 Mesoscale Patterns of Trade-Wind Clouds on Environmental Conditions. *Geophysical Research
416 Letters*, *47*(7), e2019GL085988. doi: 10.1029/2019GL085988
- 417 Bony, S., Stevens, B., Ament, F., Bigorre, S., Chazette, P., Crewell, S., ... Wirth, M. (2017).
418 EUREC4A: A Field Campaign to Elucidate the Couplings Between Clouds, Convection and
419 Circulation. *Surveys in Geophysics*, *38*(6), 1529–1568. doi: 10.1007/s10712-017-9428-0
- 420 Bretherton, C. S., & Blossey, P. N. (2017). Understanding Mesoscale Aggregation of Shallow
421 Cumulus Convection Using Large-Eddy Simulation. *Journal of Advances in Modeling Earth
422 Systems*, *9*(8), 2798–2821. doi: 10.1002/2017MS000981
- 423 Byers, H. R., & Hall, R. K. (1955, April). A CENSUS OF CUMULUS-CLOUD HEIGHT VERSUS
424 PRECIPITATION IN THE VICINITY OF PUERTO RICO DURING THE WINTER AND
425 SPRING OF 1953-1954. *Journal of the Atmospheric Sciences*, *12*(2), 176–178. doi: 10.1175/
426 1520-0469(1955)012<0176:ACOCCH>2.0.CO;2
- 427 Cooper, W. A., Lasher-Trapp, S. G., & Blyth, A. M. (2013, June). The Influence of Entrainment
428 and Mixing on the Initial Formation of Rain in a Warm Cumulus Cloud. *Journal of the
429 Atmospheric Sciences*, *70*(6), 1727–1743. doi: 10.1175/JAS-D-12-0128.1
- 430 Denby, L. (2020). Discovering the Importance of Mesoscale Cloud Organization Through Unsuper-
431 vised Classification. *Geophysical Research Letters*, *47*(1), 1–10. doi: 10.1029/2019GL085190
- 432 Dipankar, A., Stevens, B., Heinze, R., Moseley, C., Zängl, G., Giorgetta, M., & Brdar, S. (2015).
433 Large eddy simulation using the general circulation model ICON. *Journal of Advances in
434 Modeling Earth Systems*, *7*(3), 963–986. doi: 10.1002/2015MS000431
- 435 Feingold, G., McComiskey, A., Rosenfeld, D., & Sorooshian, A. (2013). On the relationship between
436 cloud contact time and precipitation susceptibility to aerosol. *Journal of Geophysical Research:
437 Atmospheres*, *118*(18), 10,544–10,554. doi: 10.1002/jgrd.50819
- 438 Freud, E., & Rosenfeld, D. (2012). Linear relation between convective cloud drop number concen-
439 tration and depth for rain initiation. *Journal of Geophysical Research: Atmospheres*, *117*(D2).
440 doi: 10.1029/2011JD016457
- 441 George, G., Stevens, B., Bony, S., Vogel, R., & Naumann, A. K. (2022). Ubiquity of shallow
442 mesoscale circulations in the trades and their influence on moisture variance. *accepted in
443 principle for Nat. Geosci.* doi: 10.1002/essoar.10512427.1
- 444 Hagen, M., Ewald, F., Groß, S., Oswald, L., Farrell, D. A., Forde, M., ... Hall, K. (2021, December).
445 Deployment of the C-band radar Poldirad on Barbados during EUREC⁴A. *Earth System
446 Science Data*, *13*(12), 5899–5914. doi: 10.5194/essd-13-5899-2021
- 447 Janssens, M., Vilà-Guerau de Arellano, J., Scheffer, M., Antonissen, C., Siebesma, A. P., & Glass-
448 meier, F. (2021). Cloud Patterns in the Trades Have Four Interpretable Dimensions. *Geo-
449 physical Research Letters*, *48*(5), e2020GL091001. doi: 10.1029/2020GL091001
- 450 Klocke, D., Brueck, M., Hohenegger, C., & Stevens, B. (2017). Rediscovery of the doldrums in
451 storm-resolving simulations over the tropical Atlantic /704/106 /704/106/35 /704/106/35/823

- 452 perspective. *Nature Geoscience*, *10*(12), 891–896. doi: 10.1038/s41561-017-0005-4
- 453 Langhans, W., Yeo, K., & Romps, D. M. (2015, March). Lagrangian Investigation of the Precipita-
 454 tion Efficiency of Convective Clouds. *Journal of the Atmospheric Sciences*, *72*(3), 1045–1062.
 455 doi: 10.1175/JAS-D-14-0159.1
- 456 Lau, K. M., & Wu, H. T. (2003). Warm rain processes over tropical oceans and climate implications.
 457 *Geophysical Research Letters*, *30*(24), 2–6. doi: 10.1029/2003GL018567
- 458 Louf, V., Jakob, C., Protat, A., Bergemann, M., & Narsey, S. (2019). The Relationship of Cloud
 459 Number and Size With Their Large-Scale Environment in Deep Tropical Convection. *Geo-
 460 physical Research Letters*, *46*(15), 9203–9212. doi: 10.1029/2019GL083964
- 461 Lutsko, N. J., & Cronin, T. W. (2018, November). Increase in Precipitation Efficiency With
 462 Surface Warming in Radiative-Convective Equilibrium. *Journal of Advances in Modeling Earth
 463 Systems*, *10*(11), 2992–3010. doi: 10.1029/2018MS001482
- 464 Mapes, B., & Neale, R. (2011). Parameterizing Convective Organization to Escape the Entrainment
 465 Dilemma. *Journal of Advances in Modeling Earth Systems*, *3*(2). doi: 10.1029/2011MS000042
- 466 Muller, C., & Takayabu, Y. (2020, March). Response of precipitation extremes to warming: What
 467 have we learned from theory and idealized cloud-resolving simulations, and what remains to
 468 be learned? *Environmental Research Letters*, *15*(3), 035001. doi: 10.1088/1748-9326/ab7130
- 469 Narenpitak, P., Kazil, J., Yamaguchi, T., Quinn, P., & Feingold, G. (2021). From Sugar to Flowers:
 470 A Transition of Shallow Cumulus Organization During ATOMIC. *Journal of Advances in
 471 Modeling Earth Systems*, *13*(10), e2021MS002619. doi: 10.1029/2021MS002619
- 472 Naumann, A. K., & Seifert, A. (2016). Recirculation and growth of raindrops in simulated shallow
 473 cumulus. *Journal of Advances in Modeling Earth Systems*, *8*(2), 520–537. doi: 10.1002/
 474 2016MS000631
- 475 Nuijens, L., & Siebesma, A. P. (2019). Boundary Layer Clouds and Convection over Subtropical
 476 Oceans in our Current and in a Warmer Climate. *Current Climate Change Reports*, *5*(2),
 477 80–94. doi: 10.1007/s40641-019-00126-x
- 478 Nuijens, L., Stevens, B., & Siebesma, A. P. (2009, July). The environment of precipitating shallow
 479 cumulus convection. *Journal of the Atmospheric Sciences*, *66*(7), 1962–1979. doi: 10.1175/
 480 2008JAS2841.1
- 481 Orlanski, I. (1975). A Rational Subdivision of Scales for Atmospheric Processes. *Bulletin of
 482 the American Meteorological Society*, *56*(5), 527–530. Retrieved 2023-07-21, from [https://
 483 www.jstor.org/stable/26216020](https://www.jstor.org/stable/26216020)
- 484 Radtke, J., Naumann, A. K., Hagen, M., & Ament, F. (2022, May). The relationship between
 485 precipitation and its spatial pattern in the trades observed during EUREC⁴A. *Quarterly
 486 Journal of the Royal Meteorological Society*, qj.4284. doi: 10.1002/qj.4284
- 487 Rauber, R. M., Stevens, B., Ochs, H. T., Knight, C., a. Albrecht, B., Blyth, a. M., ... Jensen,
 488 J. B. (2007). Over the ocean: The RICO campaign. *Bulletin of the American Meteorological
 489 Society*(December 2007), 1912–1928. doi: 10.1175/BAMS-88-12-1912
- 490 Rogers, R. R., & Yau, M. K. (1996). *A short course in cloud physics* (3. ed., reprint ed.) (No. 113).
 491 Woburn, Mass.: Butterworth Heinemann.
- 492 Sarkar, M., Bailey, A., Blossey, P., de Szoeko, S. P., Noone, D., Quinones Melendez, E., ... Chuang,
 493 P. (2022, November). Sub-cloud Rain Evaporation in the North Atlantic Ocean. *EGUsphere*,
 494 1–37. doi: 10.5194/egusphere-2022-1143
- 495 Schulz, H., Eastman, R., & Stevens, B. (2021). Characterization and Evolution of Organized Shal-

- 496 low Convection in the Downstream North Atlantic Trades. *Journal of Geophysical Research:*
 497 *Atmospheres*, 126(17), e2021JD034575. doi: 10.1029/2021JD034575
- 498 Schulz, H., & Stevens, B. (2023, February). On the representation of shallow convection in the
 499 trades by large-domain, hecto-meter, large-eddy simulations. *submitted to JAMES, preprint:*
 500 <https://eartharxiv.org/repository/view/4986/>.
- 501 Seifert, A., & Beheng, K. D. (2001, October). A double-moment parameterization for simulating
 502 autoconversion, accretion and selfcollection. *Atmospheric Research*, 59–60, 265–281. doi:
 503 10.1016/S0169-8095(01)00126-0
- 504 Seifert, A., & Beheng, K. D. (2006, February). A two-moment cloud microphysics parameterization
 505 for mixed-phase clouds. Part 1: Model description. *Meteorology and Atmospheric Physics*,
 506 92(1-2), 45–66. doi: 10.1007/s00703-005-0112-4
- 507 Seifert, A., & Heus, T. (2013). Large-eddy simulation of organized precipitating trade wind cumulus
 508 clouds. *Atmospheric Chemistry and Physics*, 13(11), 5631–5645. doi: 10.5194/acp-13-5631
 509 -2013
- 510 Seifert, A., & Stevens, B. (2010, May). Microphysical Scaling Relations in a Kinematic Model of
 511 Isolated Shallow Cumulus Clouds. *Journal of the Atmospheric Sciences*, 67(5), 1575–1590.
 512 doi: 10.1175/2009JAS3319.1
- 513 Short, D. A., & Nakamura, K. (2000). TRMM radar observations of shallow precipitation over
 514 the tropical oceans. *Journal of Climate*, 13(23), 4107–4124. doi: 10.1175/1520-0442(2000)
 515 013<4107:TROOSP>2.0.CO;2
- 516 Siebesma, A. P. (1998). Shallow Cumulus Convection. In E. J. Plate, E. E. Fedorovich, D. X. Viegas,
 517 & J. C. Wyngaard (Eds.), *Buoyant Convection in Geophysical Flows* (pp. 441–486). Dordrecht:
 518 Springer Netherlands. doi: 10.1007/978-94-011-5058-3_19
- 519 Snodgrass, E. R., Di Girolamo, L., & Rauber, R. M. (2009). Precipitation characteristics of trade
 520 wind clouds during RICO derived from Radar, Satellite, and aircraft measurements. *Journal*
 521 *of Applied Meteorology and Climatology*, 48(3), 464–483. doi: 10.1175/2008JAMC1946.1
- 522 Stevens, B. (2005). Atmospheric Moist Convection. *Annual Review of Earth and Planetary Sciences*,
 523 33(1), 605–643. doi: 10.1146/annurev.earth.33.092203.122658
- 524 Stevens, B., Bony, S., Brogniez, H., Hentgen, L., Hohenegger, C., Kiemle, C., ... Zuidema, P.
 525 (2020, January). Sugar, gravel, fish and flowers: Mesoscale cloud patterns in the trade winds.
 526 *Quarterly Journal of the Royal Meteorological Society*, 146(726), 141–152. doi: 10.1002/
 527 qj.3662
- 528 Stevens, B., Bony, S., Farrell, D., Ament, F., Blyth, A., Fairall, C., ... Zöger, M. (2021, August).
 529 EUREC⁴A. *Earth System Science Data*, 13(8), 4067–4119. doi: 10.5194/essd-13-4067-2021
- 530 Sui, C.-H., Satoh, M., & Suzuki, K. (2020). Precipitation Efficiency and its Role in Cloud-Radiative
 531 Feedbacks to Climate Variability. *Journal of the Meteorological Society of Japan. Ser. II*,
 532 98(2), 261–282. doi: 10.2151/jmsj.2020-024
- 533 Tompkins, A. M., & Semie, A. G. (2017). Organization of tropical convection in low vertical wind
 534 shears: Role of updraft entrainment. *Journal of Advances in Modeling Earth Systems*, 9(2),
 535 1046–1068. doi: 10.1002/2016MS000802
- 536 Touzé-Peiffer, L., Vogel, R., & Rochetin, N. (2022, May). Cold Pools Observed during EUREC4A:
 537 Detection and Characterization from Atmospheric Soundings. *Journal of Applied Meteorology*
 538 *and Climatology*, 61(5), 593–610. doi: 10.1175/JAMC-D-21-0048.1
- 539 vanZanten, M. C., Stevens, B., Nuijens, L., Siebesma, A. P., Ackerman, A. S., Burnet, F., ...

- 540 Wyszogrodzki, A. (2011, February). Controls on precipitation and cloudiness in simulations
541 of trade-wind cumulus as observed during RICO. *Journal of Advances in Modeling Earth*
542 *Systems*, *3*(2), n/a-n/a. doi: 10.1029/2011MS000056
- 543 Vial, J., Dufresne, J. L., & Bony, S. (2013). On the interpretation of inter-model spread in CMIP5
544 climate sensitivity estimates. *Climate Dynamics*, *41*(11-12), 3339–3362. doi: 10.1007/s00382
545 -013-1725-9
- 546 Vogel, R., Konow, H., Schulz, H., & Zuidema, P. (2021, November). A climatology of trade-wind
547 cumulus cold pools and their link to mesoscale cloud organization. *Atmospheric Chemistry*
548 *and Physics*, *21*(21), 16609–16630. doi: 10.5194/acp-21-16609-2021
- 549 Yamaguchi, T., Feingold, G., & Kazil, J. (2019). Aerosol-Cloud Interactions in Trade Wind Cumulus
550 Clouds and the Role of Vertical Wind Shear. *Journal of Geophysical Research: Atmospheres*,
551 *124*(22), 12244–12261. doi: 10.1029/2019JD031073
- 552 Zängl, G., Reinert, D., Rípodas, P., & Baldauf, M. (2015). The ICON (ICOsahedral Non-hydrostatic)
553 modelling framework of DWD and MPI-M: Description of the non-hydrostatic dynamical core.
554 *Quarterly Journal of the Royal Meteorological Society*, *141*(687), 563–579. doi: 10.1002/
555 qj.2378